

The effect of organic anion-transporting polypeptides 1B1, 1B3 and 2B1 on the antitumor activity of flavopiridol in breast cancer cells

STEFAN BRENNER¹, JULIANE RIHA¹, BENEDIKT GIESSRIGL¹, THERESIA THALHAMMER²,
MICHAEL GRUSCH³, GEORG KRUPITZA⁴, BRUNO STIEGER⁵ and WALTER JÄGER¹

¹Department of Clinical Pharmacy and Diagnostics, University of Vienna, Vienna; ²Department of Pathophysiology and Allergy Research, Center of Pathophysiology, Medical University of Vienna; ³Department of Medicine I, Division of Cancer Research, Medical University of Vienna; ⁴Clinical Pathology, Medical University of Vienna, Vienna, Austria; ⁵Department of Clinical Pharmacology and Toxicology, University Hospital Zurich, Zurich, Switzerland

Received August 20, 2014; Accepted September 29, 2014

DOI: 10.3892/ijo.2014.2731

Abstract. The contribution of organic anion transporting polypeptides (OATPs) to the cellular uptake of flavopiridol was investigated in OATP1B1-, OATP1B3- and OATP2B1-expressing Chinese hamster ovary (CHO) cells. Uptake of flavopiridol into these cells showed typical Michaelis-Menten kinetics with much higher transport capacity for OATP1B3 compared to OATP1B1 and OATP2B1 (V_{max}/K_m , 33.9 vs. 8.84 and 2.41 $\mu\text{l}/\text{mg}/\text{min}$, respectively). The predominant role of OATPs was further supported by a dramatic inhibition of flavopiridol uptake in the presence of the OATP substrate rifampicin. Uptake of flavopiridol by OATPs also seems to be an important determinant in breast cancer cells. The much higher mRNA level for OATP1B1 found in wild-type compared to ZR-75-1 OATP1B1 knockdown cells correlated with higher flavopiridol initial uptake leading to 4.6-fold decreased IC_{50} values in the cytotoxicity assay (IC_{50} , 1.45 vs. 6.64 μM). Cell cycle profile also showed a clear incidence for a stronger cell cycle arrest in the G2/M phase for ZR-75-1 wild-type cells compared to OATP1B1 knockdown cells, further indicating an active uptake via OATP1B1. In conclusion, our results revealed OATP1B1, OATP1B3 and OATP2B1 as uptake transporters for flavopiridol in cancer cells, which may also apply in patients during cancer therapy.

Introduction

Flavopiridol (Alvocidib, NSC 649890, (-)-cis-5,7-dihydroxy-2-(2-chlorophenyl)-8[4-(3-hydroxy-1-methyl) piperidinyl]-4H-ben-

zopyran-4-on) is a selective inhibitor of cyclin dependent kinases (CDK1, CDK2, CDK4 and CDK7) thereby blocking cell cycle progression at the G1 to S and G2 to M interface (1). Flavopiridol, therefore, exerts pronounced antitumor activity in a variety of cell types including human breast, prostate, hematopoietic, lung, head and neck cancer cells, and also in human tumor xenograft models including colon and prostate carcinomas (1-4). Clinical trials with flavopiridol as a single agent or in combination with anticancer drugs, including taxanes and gemcitabine (5,6), also showed tumor responses in most phase I (7,8) and phase II (9,10) studies on different types of progressive tumors refractory to conventional treatment. Furthermore, the overall response rate could be also increased when flavopiridol was administered as a single agent using a pharmacokinetically-directed schedule (8,10). However, still there was a high amount of variability in pharmacokinetics, response and toxicity which could not be explained by demographic, patients' and disease characteristics but might be caused by an altered flavopiridol accumulation in cancer cells. One factor strongly affecting anticancer drug concentrations thereby leading to altered response rates is metabolism. Indeed, recent data from our lab showed extensive glucuronidation of flavopiridol to the 5- and 7-hydroxy position in human liver microsomes by uridine diphosphate glucuronosyltransferase isoforms 1A1 and 1A9 (UGT1A1 and UGT1A9, respectively) (11). Polymorphic UGTs may therefore affect the extent of glucuronidation as well as flavopiridol disposition, activity and toxicity in a manner similar to irinotecan, a drug which shows pronounced glucuronidation (12-14). In fact, patients with diarrhea after flavopiridol treatment had a lower metabolic ratio (flavopiridol glucuronide/flavopiridol) than patients without diarrhea, indicating that systemic glucuronidation of flavopiridol is inversely associated with the risk of developing diarrhea. It is well established that overexpression of ATP-powered efflux pumps such as P-glycoprotein (P-gp), MDR1 and ABCB1, the breast cancer resistance protein BCRP (ABCG2) and the multidrug resistance protein MRP2 (ABCC2) have a great impact on intracellular concentrations of various anticancer agents. Indeed, flavopiridol was less toxic in CHO cells expressing higher levels of P-gp (15)

Correspondence to: Professor Walter Jäger, Department of Clinical Pharmacy and Diagnostics, University of Vienna, A-1090 Vienna, Austria
E-mail: walter.jaeger@univie.ac.at

Key words: flavopiridol, breast cancer, OATP, cellular uptake, transport, cell cycle inhibition

and in acute leukemia patients with high BCRP mRNA expression in the blast cells (16). MRP2 might indirectly also contribute to cellular drug concentrations as it is the main efflux transporter for flavopiridol glucuronides into bile where they can be cleaved by β -glucuronidase and reabsorbed (17). However, uptake mechanisms into tumor cells might be even more important than efflux transporters for the efficacy of anticancer drugs because they are determinants for intracellular drug concentration (18). One of the most important cellular drug uptake mechanisms in humans is via members of the organic anion-transporting polypeptide family (OATP) (19,20). To facilitate readability and understanding of this report, 'OATP' is used for both genes and proteins. OATPs are expressed in a variety of tissues (21) and tumors (22-24), where they mediate the transport of endogenous and exogenous compounds, including drugs (19,20,25). Studies have shown that uptake transporters can confer sensitivity to anticancer agents (26-30) such as the OATP1B3 substrates methotrexate and paclitaxel (26,31). This may be therapeutically important because expression of OATP varies greatly among tumor cell lines (32). Cellular uptake of flavopiridol is facilitated by OATP1B1 in transiently transfected HEK-293 and MDCK-II cells (33). Furthermore, Ni and coworkers (33) also identified OATP1B1_rs11045819 as a polymorphic OATP1B1 variant associated with improved flavopiridol response in relapsed chronic lymphocytic leukaemia patients. However, the authors did not investigate the kinetic parameters for the cellular uptake of flavopiridol in OATP1B1-transfected cells nor did they elucidate the impact of OATP expression on flavopiridol cytotoxicity in cancer cells. As OATPs exhibit overlapping substrate specificity, we hypothesized that additional OATPs may also contribute to the uptake of flavopiridol. In the present study, we therefore investigated the time and concentration-dependent transport of flavopiridol in stable OATP1B1-, OATP1B3- and OATP2B1-transfected CHO cells. Furthermore, the impact of OATP expression on cytotoxicity and cell cycle progression of flavopiridol-treated human breast cancer cells ZR-75-1 was also investigated.

Materials and methods

Materials. Flavopiridol (2-(2-chlorophenyl)-5,7-dihydroxy-8-[(3S,4R)-3-hydroxy-1-methyl-4-piperidinyl]-4-chromenone), was obtained from Sigma-Aldrich (Munich, Germany). Acetonitrile and water were of HPLC grade (Merck, Darmstadt, Germany). All other chemicals and solvents were commercially available, of analytical grade and used without further purification.

Cell culture. Chinese hamster ovary (CHO) cells that were stably transfected with OATP1B1, OATP1B3 or OATP2B1 and wild-type CHO cells were provided by the University of Zurich, Switzerland and have been extensively previously characterized (34,35). The CHO cells were grown in Dulbecco's modified Eagle's medium (DMEM) supplemented with 10% FCS, 50 μ g/ml L-proline, 100 U/ml penicillin and 100 μ g/ml streptomycin. The selective medium for stably transfected CHO cells additionally contained 500 μ g/ml geneticin sulfate (G418) (36). All the media and supplements were obtained from Invitrogen (Karlsruhe, Germany). The mammalian ZR-75-1 breast cancer cell line was purchased from the

American Type Culture Collection (ATCC, Rockville, MD, USA) and was maintained in RPMI medium supplemented with 10% FCS, 100 U/ml penicillin, 100 μ g/ml streptomycin and 1% GlutaMAX. The cells were grown in T-flasks with a 25 cm² growth area (BD Biosciences, Franklin Lakes, NJ, USA), maintained at 37°C under 5% CO₂ and 95% relative humidity. The cells were passaged once a week and were used up to passage 55 (37).

OATP1B1 knockdown in ZR-75-1 cells. For lentiviral transduction, ZR-75-1 cells were plated in 24-well tissue culture plates at a density of 40,000 cells/well in 0.5 ml of growth medium. After 24 h, 250 μ l of medium supplemented with 8 μ g/ml polybrene (H9268; Sigma) was added. Transductions were performed by the addition of 10 μ l of shRNA (Mission[®] transduction particles NM_006446, Sigma, TRCN0000043203, coding sequence CCGGGCCTTCATCTAAGGCTAACATCTCGAGATGTTAG-CCTTAG-ATGAAGGCTTTTGTG). Twenty-four hours after the transduction, the cell culture medium was changed, and 1 ml of growth medium supplemented with 1 or 5 μ g/ml of puromycin (P9620; Sigma) was added to select infected cells after an additional 24 h. The obtained silencing efficiency was evaluated after 3 weeks via real-time PCR and immunofluorescence (38).

Real-time RT-PCR. Total RNA was extracted from cell lines using the TRIzol reagent (Invitrogen) according to the manufacturer's instructions. The concentration, purity and integrity of the RNA samples were determined through UV absorbance and electrophoresis. Total RNA (2 μ g) were reverse transcribed to cDNA using random hexamer primers and the RevertAid[™] H Minus M-MuLV Reverse Transcriptase system (Fermentas, St. Leon-Rot, Germany), as recommended by the manufacturer. TaqMan[®] Gene Expression assays (Applied Biosystems, Warrington, UK) were purchased for human OATP1B1. The 18S gene was used as a reference gene, as previously described (23). Multiplex quantitative real-time RT-PCR was performed in an amplification mixture with a volume of 20 μ l. The target gene amplification mixture contained 10 μ l of 2X TaqMan[®] Universal PCR Master Mix, 1 μ l of the appropriate Gene Expression Assay, 1 μ l of the TaqMan[®] endogenous control (human β -actin or 18S), 10 ng of template cDNA diluted in 5 μ l of nuclease-free water and 3 μ l of nuclease free water. The thermal cycling conditions were as follows: 2 min at 50°C and 10 min at 95°C, followed by 40 cycles of 15 sec at 95°C and 1 min at 60°C. Fluorescence generation due to TaqMan[®] probe cleavage via the 5'-3' exonuclease activity of DNA polymerase was measured with the ABI PRISM 7700 Sequence Detection System (Applied Biosystems). All samples were amplified in triplicate. To cover the range of expected Ct values for the target mRNA, a standard curve of six serial dilutions from 50 ng to 500 pg of pooled cDNA was analyzed using the Sequence Detection Software (SDS 1.9.1.; Applied Biosystems). The results were imported into Microsoft Excel for further analysis. Comparable cDNA contents in the experimental samples were calculated according to the standard curve method. Relative gene expression data are given as the n-fold change in transcription of target genes normalized to the endogenous control. Real-time RT-PCR was performed with the following prefabricated TaqMan[®] Gene Expression

Assays (Applied Biosystems) containing intron-spanning primer Hs00272374_ml for OATP1B1.

Immunofluorescence. ZR-75-1 OATP1B1-knockdown cells and cells transduced with the empty vector were allowed to attach on culture slides overnight (8-Chamber Polystyrene Vessel Tissue Culture-Treated Glass Slides; BD Falcon). Formalin fixation was followed by a washing step and a blocking step (by 5% BSA). The primary antibody against OATP1B1 (OATP1B1/1B3 mMDQ mouse monoclonal antibody; Acris Antibodies, Herford, Germany) was diluted 1:100, and incubation was performed for 2 h. Optimal antibody concentrations were determined by titrating serial antibody dilutions. The applied dilutions corresponded to the minimum concentration necessary to produce a positive signal. Wild-type and OATP1B1-transfected CHO cells were used as controls. Following incubation with the secondary antibody (1:1,000 dilution; Alexa Fluor® 488 goat anti-mouse IgG; Invitrogen, Carlsbad, CA, USA) for 30 min, cell nuclei were stained with 0.5 µg/ml Hoechst 33342 (Sigma-Aldrich). Thereafter, the slides were rinsed with distilled water before being mounted in Mowiol 4-88 (Carl Roth, Karlsruhe, Germany). Fluorescent staining was visualized with an Axioplan 2 microscope (Carl Zeiss, Jena, Germany). Images were captured using a AxioCam HRc2 Color CCD digital camera and AxioVision 4.8 software (Carl Zeiss Vision GmbH, Aalen, Germany). To minimize background signals and to make the signal intensity and extension in different samples comparable, the exposure times for the individual antibodies were evaluated and kept constant between the samples (38).

Cellular uptake. Transport assays were performed on 12-well plates as described in detail elsewhere (34). Briefly, CHO cells were seeded at a density of 350,000 cells/well on 12-well plates (BD Biosciences, Franklin Lakes, NJ, USA). Uptake assays were generally performed on day 3 after seeding, when the cells had grown to confluence. Twenty-four hours before starting the transport experiments, the cells were additionally treated with 5 mM sodium butyrate (Sigma-Aldrich) to induce non-specific gene expression (39). Flavopiridol was dissolved in DMSO and was diluted with uptake buffer (pH 7.4; final DMSO concentration of 0.5%) to 25-800 µM. Control experiments contained DMSO in the medium in place of flavopiridol. Prior to the transport experiment, the cells were rinsed twice with 2 ml of prewarmed (37°C) uptake buffer (116.4 mM NaCl, 5.3 mM KCl, 1 mM NaH₂PO₄, 0.8 mM MgSO₄, 5.5 mM D-glucose and 20 mM HEPES; pH adjusted to 7.4). Uptake was initiated by adding 0.25 ml of uptake buffer containing the substrate. After the indicated time period at 37°C, uptake was stopped by removing the uptake solution and washing the cells five times with 2 ml of buffer (pH 7.4). The cells were then trypsinized by the addition of 100 µl of trypsin and transferred into test tubes. Next, the cell membranes were disrupted via repeated (5 times) shock freezing in liquid nitrogen and thawing. Following centrifugation at 13,500 x g for 5 min, 100 µl of the supernatant was diluted with methanol/water (2:1; v/v), and aliquots (80 µl) were analyzed via HPLC (37).

Inhibition analysis. For the inhibition experiments with rifampicin and bromosulfophthalein (BSP; Sigma-Aldrich),

stock solutions of these compounds were prepared in DMSO containing the indicated concentrations. CHO cells grown on 12-well plates were first washed twice with pre-warmed uptake buffer (pH 7.4) and incubated for 10 min at 37°C under 5% CO₂ with 1 µM flavopiridol in the presence of the inhibitors ranging from 0.0001 to 100 µM. Control experiments were performed without BSP and rifampicin under identical conditions as mentioned above.

Cytotoxicity assay. CellTiter-Blue (Promega, Southampton, UK) is a type of a colorimetric assay used to measure cell viability via non-specific redox enzyme activity (reduction from resazurin to resorufin by viable cells). ZR-75-1 cells (50,000 cells/ml) were seeded into 96-well flat-bottomed plates and incubated for 24 h at 37°C under 5% CO₂. For cytotoxicity assays, the cells were incubated with various concentrations of flavopiridol (5-400 µM) for 72 h. The CellTiter-Blue (20 µl) reagent was added to the wells, and the plate was incubated for 2 h, protected from light. The absorbance was recorded for resazurin (605 nm) and resorufin (573 nm). The assay results were measured on a Tecan M200 multimode plate reader (Tecan Austria GmbH, Groedig, Austria). The absorbance was also measured in CellTiter-Blue assays in blank wells (without resveratrol) and subtracted from the values from experimental wells. The viability of the treated cells was expressed as a percentage of the viability of the corresponding control cells. All experiments were repeated at least three times.

Cell cycle distribution analyses by fluorescence activated cell sorting (FACS). ZR-75-1 wild-type and OATP1B1 knockdown cells were plated on 6-well plates at a concentration of 1x10⁶ cells/ml and allowed to attach overnight. After 24 and 48 h of incubation at 37°C cells were trypsinized by the addition of 100 µl of trypsin, transferred into 15 ml tubes and centrifuged (4°C, 800 rpm, 5 min) (40). The supernatant was discarded and the cell pellet washed with cold PBS (phosphate-buffered saline, pH 7.4), centrifuged (4°C, 800 rpm, 5 min), resuspended in 1 ml cold ethanol (70%) and fixed for 30 min at 4°C. After two washing steps with cold PBS, the cell pellet was resuspended in 500 µl cold PBS and transferred into a 5 ml polystyrene round bottom tube. RNase A and propidium iodide were added to a final concentration of 50 µg/ml and incubated for 1 h at 4°C. The final cell number was adjusted between 0.5 and 1x10⁶ cells in 500 µl. Cells were analyzed by the FACSCalibur flow cytometer (BD Biosciences). Cell cycle distribution was calculated with ModFid LT software (Verity Software House, Topsham, ME, USA).

Determination of protein concentrations. Total protein was determined using the colorimetric bicinchoninic acid protein (BCA) assay kit (Pierce Science, Rockford, IL, USA) with bovine serum albumin as a standard and quantification at a wavelength of 562 nm on a spectrophotometer (UV-1800; Shimadzu). Raw data were analyzed using UVProbe software (version 2.31; Shimadzu). The protein concentrations were consistent among the plates (0.150±0.005 mg/well).

HPLC chromatography. The determination of flavopiridol was performed using a Merck 'La Chrom' System (Merck,

Table I. Uptake kinetic parameters for flavopiridol in OATP-transfected CHO and ZR-75-1 cells.

Cell lines	Km (μM)	Vmax (pmol/mg/min)	Vmax/Km ($\mu\text{l}/\text{min}\cdot\mu\text{g}$)
OATP1B1 t.f. CHO	66.0 \pm 10.3	583 \pm 19.8	8.84 \pm 0.30
OATP1B3 t.f. CHO	66.8 \pm 21.3	2263 \pm 156	33.9 \pm 0.94
OATP2B1 t.f. CHO	175 \pm 25.8	422 \pm 19.9	2.41 \pm 0.03
ZR-75-1 w.t.	80.8 \pm 14.1	1876 \pm 74.0	23.2 \pm 0.90
OATP1B1 k.d. ZR-75-1	99.0 \pm 24.0	758 \pm 44.9	7.66 \pm 0.13

Values are means \pm SD of 3 individual determinations. The net OATP-mediated uptake values were calculated by subtracting the values obtained with the wild-type (w.t.) CHO cells from those obtained with the stably transfected cells. Kinetic parameters were calculated by fitting the data to the Michaelis-Menten (Km) equation with non-linear regression. t.f., transfected; w.t., wild-type; k.d., knockdown.

Darmstadt, Germany) equipped with an L-7250 injector, an L-7100 pump, an L-7300 column oven (set at 37°C), a D-7000 interface, and a L-7400 UV detector (set at a wavelength at 264 nm). Chromatographic separation of flavopiridol was performed on a Hypersil BDS C18 Column (5 μM , 250 x 4.6 mm I.D.; Thermo Electron Corp.), preceded by a Hypersil BDS C18 precolumn (5 μM , 10 x 4.6 mm I.D.) at a flow rate of 1 ml/min. The mobile phase consisted of a continuous linear gradient, mixed from 10 mM ammonium acetate/acetic acid buffer, pH 7.4 (mobile phase A), and acetonitrile (mobile phase B), to elute flavopiridol. The mobile phase was filtered through a 0.45 μM filter (HVLPO4700; Millipore, Vienna, Austria). The gradient ranged from 10% acetonitrile (0 min) to 40% B at 15 min and linearly increased to 80% B at 17 min where it remained constant for 23 min. Subsequently, the percentage of acetonitrile was decreased within 3 min to 10% in order to equilibrate the column for 9 min before application of the next sample. The sample injection volume was 80 μl . Calibration of the chromatogram was accomplished using the external standard method by spiking drug-free cell culture medium with standard solutions of flavopiridol to give a concentration range of 0.005-1 $\mu\text{g}/\text{ml}$ (average correlation coefficient: >0.999). For this method the lower limit of quantification for flavopiridol was 10 ng/ml. Coefficients of accuracy and precision for this compound were <9.8%.

Data analysis. Kinetic analysis of the uptake of flavopiridol was performed over a substrate concentration range of 25-800 μM . Prior to these experiments, the linearity of cellular uptake over time (1, 3 and 10 min) was individually determined for wild-type and OATP-transfected CHO cells by using flavopiridol (50 μM) as a substrate. Cellular uptake rates are presented after normalization for the incubation time and total protein content. Net uptake rates were calculated as the difference in the uptake rate of the transfected and wild-type cells for each individual concentration. The data were fitted to the Michaelis-Menten model. Kinetic parameters were calculated using the GraphPad Prism Version 5.0 software program (GraphPad Software, San Diego, CA, USA) for Michaelis-Menten: $V = V_{\text{max}} * S / (K_{\text{m}} + S)$, where V is the rate of the reaction, Vmax is the maximum velocity, Km is the Michaelis constant and S is the substrate concentration. The intrinsic clearance, which is defined as the ratio Vmax/Km, quantifies the transport capacity. IC₅₀ values were determined by plotting

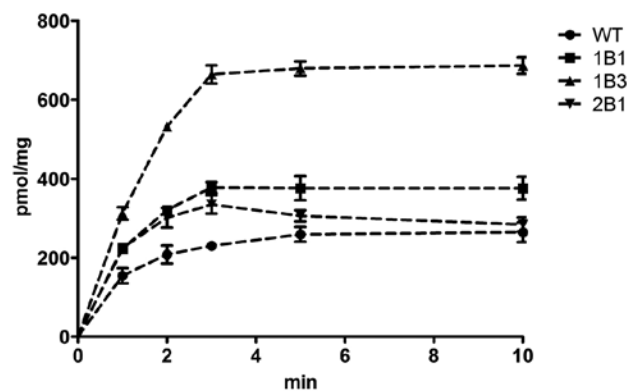


Figure 1. Time-dependent uptake of flavopiridol in OATP-transfected CHO cells. The uptake of flavopiridol (10 μM) after 1, 2, 3, 5 and 10 min was determined in wild-type and OATP1B1-, OATP1B3- and OATP2B1-transfected CHO cells at pH 7.4, 37°C. The data represent the mean \pm SD of 3 individual determinations.

the log inhibitor concentration against the net uptake rate and non-linear regression of the dataset using the equation:

$$y = \frac{a}{1 + [I / (IC_{50})]^s + b}$$

in which y is the net uptake rate (pmol/ μg protein/min), I is the inhibitor concentration (μM), s is the slope at the point of inversion, and a and b are the maximum and minimum values for cellular uptake. Net uptake was calculated for each inhibitor concentration as the difference in the uptake rates of the transporter-expressing and wild-type cell lines. Unless otherwise indicated, values are expressed as mean \pm SD of three individual experiments. Significant differences from control values were determined using a Student's paired t-test at a significance level of P<0.05.

Results

Uptake kinetics of flavopiridol in OATP transfected CHO cells. To investigate whether OATPs other than OATP1B1 contribute to flavopiridol uptake respective studies were performed in CHO cells transfected with OATP1B1, OATP1B3 and OATP2B1 using wild-type CHO cells transfected with the empty vector as controls. Western blot analysis confirmed

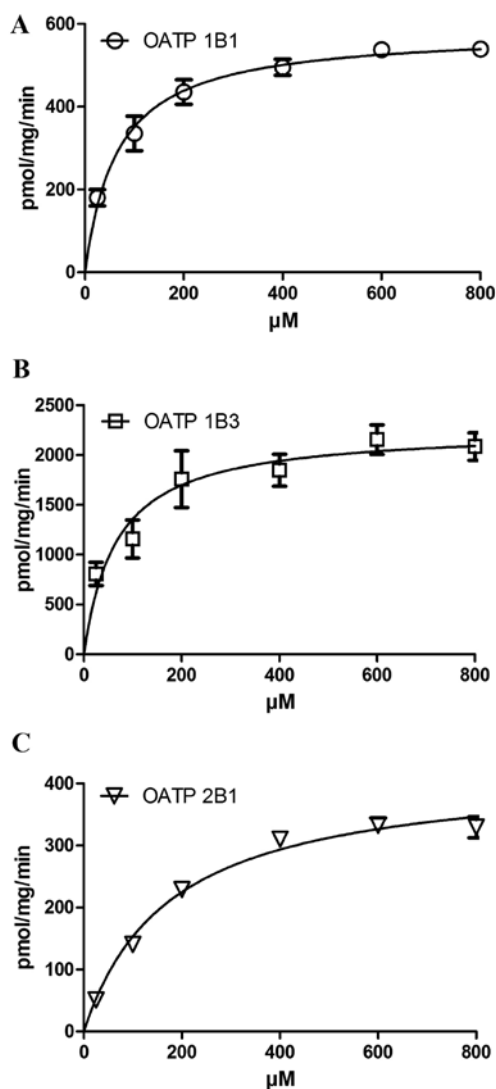


Figure 2. Uptake of flavopiridol in OATP-transfected and wild-type CHO cells. The uptake of flavopiridol (25-800 μM) by (A) OATP1B1-, (B) OATP1B3- and (C) OATP2B1-transfected CHO cells and wild-type CHO cells was determined after 1 min at pH 7.4, 37°C. After the uptake into wild-type cells was subtracted, net-OATP1B1, OATP1B3 and OATP2B1-mediated uptake was fitted to the Michaelis-Menten equation to calculate K_m and V_{max} values. The data represent the mean \pm SD of 3 individual determinations.

that these cells highly expressed the respective transporters in the membranes (data not shown). Uptake of flavopiridol (25-800 μM) for all three OATPs was only linear for up to 1 min (Fig. 1). We therefore finalized all experiments at the initial linear phase. As shown in Table I and Fig. 2, the initial net OATP1B1-, OATP1B3- and OATP2B1-mediated accumulation rates (transfected wild-type) for flavopiridol followed Michaelis-Menten kinetics, with ~4-5-fold higher V_{max} values for OATP1B3 compared to OATP1B1 and OATP2B1 (V_{max} , 2263 vs. 583 and 422 pmol/mg protein/min). The affinity of flavopiridol for both OATP1B1 and OATP1B3 showed very similar K_m values (66.0 and 66.8 μM) but was significantly higher for OATP2B1 (175 μM).

Effect of OATP inhibitors on the accumulation of flavopiridol in transfected CHO cells. To investigate whether

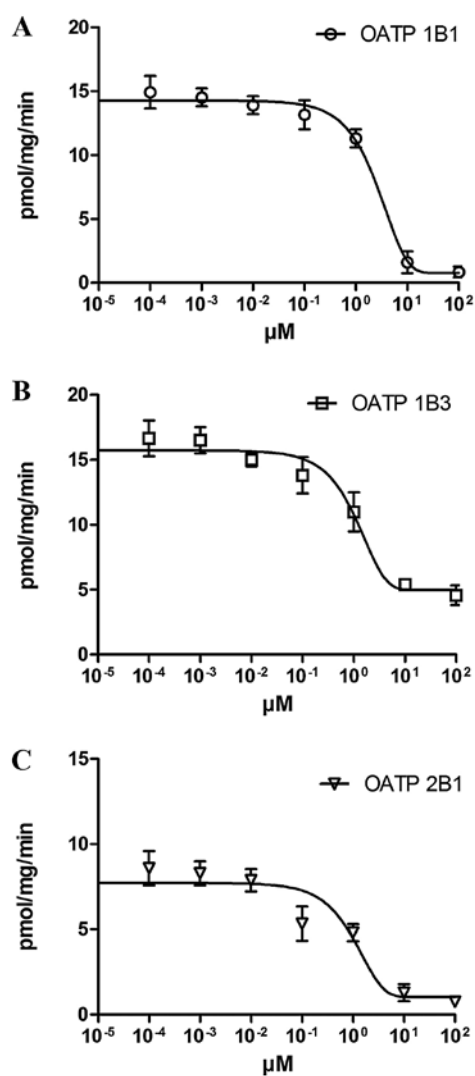


Figure 3. Inhibition of flavopiridol uptake into OATP-transfected and wild-type CHO cells by rifampicin. (A) OATP1B1-, (B) OATP1B3- and (C) OATP2B1-transfected CHO cell were co-incubated with 1 μM flavopiridol and increasing concentrations of rifampicin (0.0001-10 μM) at 37°C for 1 min (Materials and methods). Values are expressed as a percentage of vehicle control; each value represents the mean \pm SD of three independent experiments.

known OATP inhibitors impact OATP1B1-, OATP1B3- and OATP2B1-mediated flavopiridol accumulation, flavopiridol was quantified after treatment of OATP1B1-, OATP1B3- and OATP2B1-overexpressing CHO cells with 1 μM flavopiridol in the absence and presence of increasing concentrations of the known OATP inhibitors bromsulphophthalein (BSP) and rifampicin (41,42). As shown in Fig. 3 rifampicin was a potent inhibitor for flavopiridol uptake in OATP1B3- followed by OATP2B1- and OATP1B1-transfected CHO cells (IC_{50} values, 1.00, 1.36 and 2.06 μM , respectively). BSP, however, did not inhibit but rather stimulated OATP-dependent flavopiridol uptake at concentrations up to 100 μM .

OATP1B1 knockdown in ZR-75-1 cells. The cells exhibiting the lowest expression of OATP1B1 (relative mRNA expression was reduced from 14.8 \pm 0.26 to 1.19 \pm 0.02) were chosen for further experiments. Because ZR-75-1 cells express OATP1B1 (23) but not OATP1B3 and OATP2B1, the expression of the OATP1B1

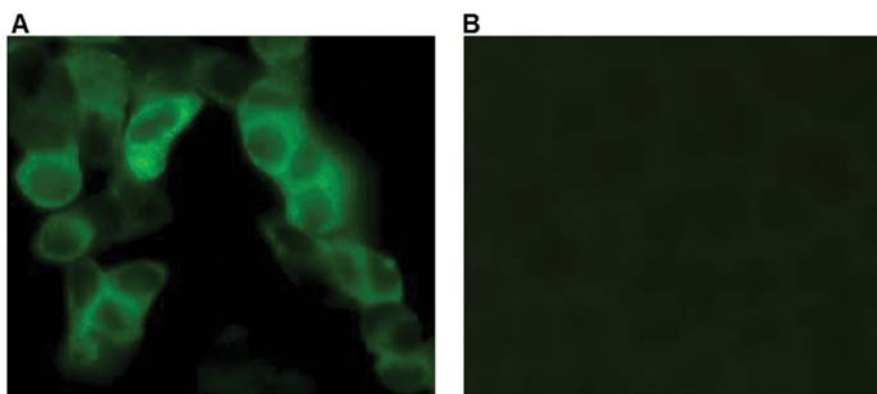


Figure 4. Immunofluorescent characterization of OATP1B1 in ZR-75-1 and OATP1B1 knockdown ZR-75-1 cells. Cells were grown on culture slides and stained with an antibody against OATP1B1 (Materials and methods). Immunofluorescence was performed in ZR-75-1 empty vector-transfected cells (A) and ZR-75-1 OATP1B1 knockdown cells (B). Bright green fluorescence was seen in ZR-75-1 empty vector-transfected cells.

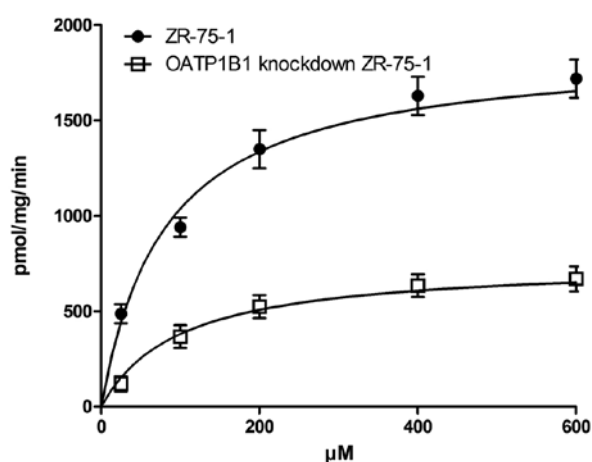


Figure 5. Uptake of flavopiridol in ZR-75-1 and OATP1B1 knockdown ZR-75-1 cells. The uptake of flavopiridol (25–600 μM) in ZR-75-1 empty vector-transfected and OATP1B1 knockdown ZR-75-1 cells was determined after 1 min at pH 7.4, 37°C and the OATP-mediated uptake was fitted to the Michaelis-Menten equation to calculate K_m and V_{max} values. Data represent the mean ± SD of triplicate determination.

protein was furthermore confirmed by immunofluorescence. Fig. 4 clearly shows constitutive expression (bright green fluorescence) of OATP1B1 in ZR-75-1 control cells (transfected with empty vector) (Fig. A) and suppressed protein levels of this transporter in ZR-75-1 OATP1B1-knockdown cells (Fig. B).

Uptake kinetics of flavopiridol in wild-type and OATP1B1 knockdown ZR-75-1 cells. Based on much higher OATP1B1 expression levels in wild-type ZR-75-1 breast cancer cell lines compared to OATP1B1 knockdown ZR-75-1 cells, we expected increased intracellular flavopiridol levels in the wild-type cells. For kinetic analysis, an incubation time of 1 min was chosen in order to prevent cellular uptake from interference with cellular efflux mechanisms such as MRP1 and BCRP. Fig. 5 depicts representative Michaelis-Menten kinetics for a significantly higher flavopiridol uptake (2.5-fold) by wild-type compared to OATP1B1 knockdown ZR-75-1 cells (V_{max} , 1876 pmol/mg vs. 758 pmol/mg). Affinity of flavopiridol to OATP1B1, however, was comparable in wild-type and OATP1B1 knockdown ZR-75-1 cells (K_m , 80.8 μM±14.1 and 99.0 μM±24.0)

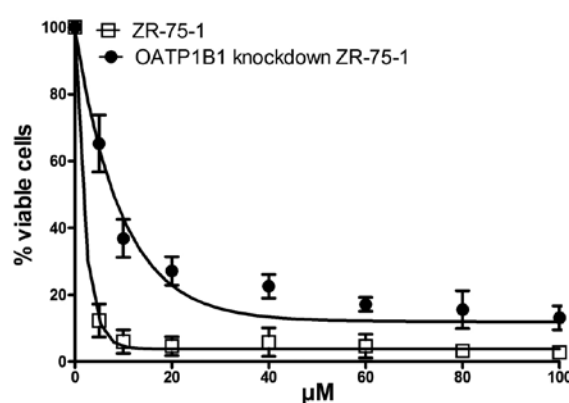


Figure 6. Cytotoxicity of flavopiridol to ZR-75-1 and OATP1B1 knockdown ZR-75-1 cells. After incubation for 72 h with 5–600 μM flavopiridol at 37°C percent viable cells were determined (Materials and methods). Dose response curves were obtained by non-linear curve fitting using the GraphPad Prism 5.0 program. The data represent the mean ± SD of 3 individual determinations.

indicating that OATP1B1 knockdown did not unmask other transporters for flavopiridol.

Cytotoxicity of flavopiridol in wild-type and OATP1B1 knockdown ZR-75-1 cells. The cytotoxicity of flavopiridol against ZR-75-1 and OATP1B1 knockdown ZR-75-1 breast cancer cells was quantified using the CellTiter-Blue test kit. As shown in Fig. 6, flavopiridol was significantly less toxic in OATP1B1 knockdown (IC_{50} , 6.64 μM) than in wild-type ZR-75-1 cells (IC_{50} , 1.45 μM) underscoring that OATP1B1 is important for flavopiridol uptake.

Effect of flavopiridol on the cell cycle of ZR-75-1 wild-type and OATP1B1 knockdown cells. ZR-75-1 cells were incubated with 5 μM flavopiridol for 8, 24 and 48 h and then subjected to FACS analyses. In the absence of flavopiridol both cell lines showed a nearly identical distribution of cells in the different phases of the cell cycle (Fig. 7). Addition of flavopiridol, however, exhibited distinct effects dependent on OATP1B1 expression. While the cell cycle of wild-type cells was inhibited in G1 and G2/M phase, OATP1B1-knockdown cells were inhibited only in G1 phase at the expense of G2/M- and S-phase cells after

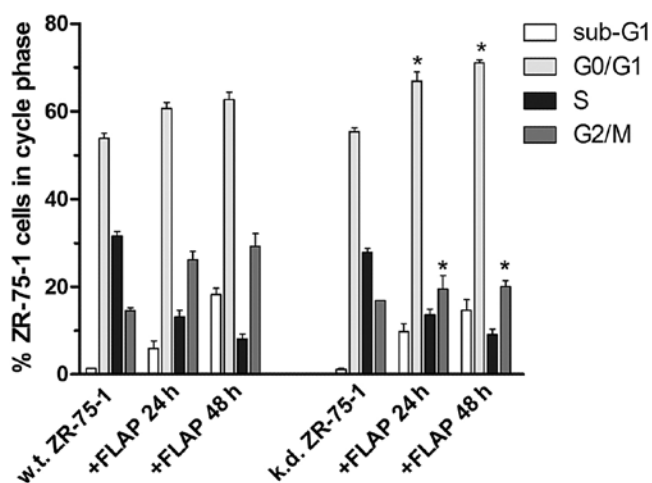


Figure 7. Analysis of cell cycle distribution in wild-type and OATP1B1 knockdown ZR-75-1 cells. ZR-75-1 cells (1×10^6 cells/ml) with flavopiridol ($10 \mu\text{M}$), harvested after 24 and 48 h, and subjected to FACS analysis. Error bars indicate \pm SD, and asterisk significant alterations of cell distributions in the respective cell cycle phase compared to control ($P < 0.05$). Experiments were performed in triplicate.

24 and 48 h of flavopiridol treatment. Notably, reduced uptake of flavopiridol in OATP1B1 knockdown cells was also associated with a decreased proportion of cells in sub-G1 indicating decreased induction of apoptosis observed after 48 h of flavopiridol incubation (14.5 compared to 18.2% for wild-type cells).

Discussion

In the present study, we identified the human OATP isoforms responsible for the cellular uptake of flavopiridol and demonstrated the relevance of flavopiridol uptake for its anticancer activity. To date, the only OATP that has been characterized, by Ni *et al* (33), as an uptake transporter for flavopiridol is the OATP1B1. Furthermore, expression of the polymorphic variant OATP1B1_rs11045819 was associated with improved flavopiridol response in patients with chronic lymphatic leukemia (33). By systematically investigating the transport properties of flavopiridol for other OATPs using the transfected CHO cells as an *in vitro* model, we were able to identify OATP1B3 and OATP2B1 as additional uptake transporters for flavopiridol. As shown in Fig. 2 and Table I, flavopiridol exhibited saturable uptake kinetics for OATP1B1, OATP1B3 and OATP2B1. The affinity of flavopiridol for OATP1B1 and OATP1B3 was similar (K_m s, 66.0 and 66.8 μM) but 2.6-fold lower for OATP2B1 (K_m , 175 μM). Furthermore, uptake of flavopiridol into OATP1B3-transfected CHO cells was up to 5.3-fold higher (V_{max} , 2263 pmol/mg/min) leading to an 3.8- and 14-fold increased transport capacity for OATP1B3 compared to OATP1B1 and OATP2B1 (V_{max}/K_m s, 33.9 vs. 8.84 and 2.41 $\mu\text{l}/\text{min}/\text{mg}$ protein, respectively; Table I) indicating that OATP1B3 might be the far most important uptake transporter for flavopiridol followed equally by OATP1B1 and OATP2B1.

Our data also suggest that OATP1B1, OATP1B3 and OATP2B1 are low affinity transporters and that the blood concentration of flavopiridol is considerably lower than the K_m values. Indeed, administration of the standard dose of flavopiridol ($50 \text{ g}/\text{m}^2$) as a 4-h infusion dose to patients with relapsed,

symptomatic CLL or small lymphocytic lymphoma (SLL) in phase I and II studies showed peak plasma concentrations of $\sim 3 \mu\text{M}$ (43). Despite this low substrate concentration relative to the K_m value, uptake of flavopiridol into cancer cells is most likely pharmacodynamically effective but slow. It should be kept in mind that the local concentrations at the cancer cells are unknown, and other parameters like local pH (36) may also affect the transport rate of the OATPs expressed in cancer cells. In addition, extrapolating *in vitro* results to the *in vivo* situation should be done with care as the absolute amount of OATP transporters in cancer cells may vary and as it is not known yet whether other transporters like OATP2A1 and OATP4C1 which are expressed in ZR-75-1 wild-type cells (23) are also involved in the uptake of flavopiridol. Other possible candidates may be organic anion transporters (OATs). Besides numerous clinically used drugs, OATs are also involved in the transport of polyphenol conjugates (44).

To further prove the importance of OATP1B1 for the uptake of flavopiridol, hormone-dependent ZR-75-1 cells that were previously shown to express high levels of OATP1B1, but not OATP1B3 and OATP2B1 (45), were incubated for 1 min with increasing concentrations of flavopiridol. Indeed, the uptake of flavopiridol by the ZR-75-1 OATP1B1-knockdown cells was significantly reduced compared to control cells, as indicated by lower V_{max} values (Fig. 5 and Table I). Concomitant with the decreased uptake of flavopiridol detected in OATP1B1 knockdown cells, its cytotoxicity decreased 4.6-fold (Fig. 6). The pan-CDK inhibitor flavopiridol blocks the ATP pocket of CDKs and inhibits MCF-7 and MDA-MB-468 breast cancer cells simultaneously in the G1 and G2/M phases (46). Also wild-type ZR-75-1 breast cancer cells were inhibited in G1 and G2/M, whereas knockdown cells were arrested only in the G1 phase upon flavopiridol treatment. This indicated that G1-specific CDKs, such as CDK4/6, were inhibited at lower flavopiridol concentrations (which was the case in OATP1B1 knockdown cells) compared to CDKs that are specific for the G2/M phase or required for both G1 and G2 transit (i.e. CDK1 or CDK2, respectively). Furthermore, we also observed a significantly decreased proportion of cells in the sub-G1 phase (a marker for cell debris occurring throughout cell death) after 48 h of flavopiridol treatment in OATP1B1 knockdown cells. As apoptosis is known to be induced by flavopiridol (47) decreased apoptosis rates again support the role of OATP1B1-dependent flavopiridol uptake for cytotoxicity.

OATP1B1-, OATP1B3- and OATP2B1-mediated flavopiridol transport may be of clinical importance, as all three transporters are expressed in various tumor entities including colorectal, liver, ovarian, pancreatic and prostate cancer tissues (48). Any variations in OATP expression may significantly alter the uptake of flavopiridol into targeted cells and tissues, thereby strongly affecting the efficacy of treatment. Patients with low expression of wild-type OATP1B1, OATP1B3 and OATP2B1 or patients carrying polymorphic OATP alleles may therefore show decreased response. Concomitant administration of OATP inhibitors may also interfere with the uptake of flavopiridol, leading to transporter-mediated drug/drug interactions. Our data demonstrated that rifampicin effectively inhibited flavopiridol uptake in CHO cells, mediated by OATP1B1, OATP1B3 and OATP2B1 (IC_{50} values, 0.48-1.47 μM). Additional potential inhibitors include

clarithromycin, erythromycin and roxithromycin, which inhibit the uptake of pravastatin in OATP1B1- and OATP1B3-transfected HEK293 cells (showing IC_{50} values of 32-37 μ M) (49). Moreover, cyclosporine A significantly decreases the OATP1B1- and OATP1B3-mediated uptake of bosentan (35) and fexofenadine (50) in HEK293 and CHO cells. In addition to clinically applied drugs, naturally occurring flavonoids also interfere with the OATP uptake of dehydroepiandrosterone (DHEAS), thus indicating that they constitute a novel class of OATP1B1 modulators (51). Whether all these potential OATP-dependent inhibitors interfere with the flavopiridol uptake in tumor cells is not yet known, however, care should be taken if patients use these drugs in combination with flavopiridol. Ongoing studies are verifying the interactions of drugs and dietary supplements with the OATP1B1-, OATP1B3- and OATP2B1-mediated uptake of flavopiridol.

In conclusion, our data revealed that OATP1B1, OATP1B3 and OATP2B1 act as transporters for flavopiridol; this role may also apply for the uptake of this compound into human cancer cells. Future *in vivo* studies should focus not only on the concentration of flavopiridol in target tissues but also on the expression levels of OATPs.

Acknowledgements

The present study was supported by the grant 'BioProMotion' Bioactivity and Metabolism from the University of Vienna, Austria.

References

- Carlson B, Lahusen T, Singh S, *et al*: Down-regulation of cyclin D1 by transcriptional repression in MCF-7 human breast carcinoma cells induced by flavopiridol. *Cancer Res* 59: 4634-4641, 1999.
- Sedlacek HH, Czech J, Naik R, *et al*: Flavopiridol (L86 8275; NSC 649890), a new kinase inhibitor for tumor therapy. *Int J Oncol* 9: 1143-1168, 1996.
- Czech J, Hoffmann D, Naik R and Sedlacek HH: Antitumoral activity of flavone L-86-8275. *Int J Oncol* 6: 31-36, 1995.
- Lam LT, Pickeral OK, Peng AC, *et al*: Genomic-scale measurement of mRNA turnover and the mechanisms of action of the anti-cancer drug flavopiridol. *Genome Biol* 2: Research0041, 2001.
- Reiner T, de las Pozas A and Perez-Stable C: Sequential combinations of flavopiridol and docetaxel inhibit prostate tumors, induce apoptosis, and decrease angiogenesis in the Ggamma/T-15 transgenic mouse model of prostate cancer. *Prostate* 66: 1487-1497, 2006.
- Jung CP, Motwani MV and Schwartz GK: Flavopiridol increases sensitization to gemcitabine in human gastrointestinal cancer cell lines and correlates with down-regulation of ribonucleotide reductase M2 subunit. *Clin Cancer Res* 7: 2527-2536, 2001.
- Byrd JC, Lin TS, Dalton JT, *et al*: Flavopiridol administered using a pharmacologically derived schedule is associated with marked clinical efficacy in refractory, genetically high-risk chronic lymphocytic leukemia. *Blood* 109: 399-404, 2007.
- Phelps MA, Lin TS, Johnson AJ, *et al*: Clinical response and pharmacokinetics from a phase I study of an active dosing schedule of flavopiridol in relapsed chronic lymphocytic leukemia. *Blood* 113: 2637-2645, 2009.
- Byrd JC, Peterson BL, Gabrilove J, *et al*: Treatment of relapsed chronic lymphocytic leukemia by 72-hour continuous infusion or 1-hour bolus infusion of flavopiridol: results from cancer and leukemia group B study 19805. *Clin Cancer Res* 11: 4176-4181, 2005.
- Lin TS, Ruppert AS, Johnson AJ, *et al*: Phase II study of flavopiridol in relapsed chronic lymphocytic leukemia demonstrating high response rates in genetically high-risk disease. *J Clin Oncol* 27: 6012-6018, 2009.
- Hagenauer B, Salamon A, Thalhammer T, *et al*: In vitro glucuronidation of the cyclin-dependent kinase inhibitor flavopiridol by rat and human liver microsomes: involvement of UDP-glucuronosyltransferases 1A1 and 1A9. *Drug Metab Dispos* 29: 407-414, 2001.
- Mani S: UGT1A1 polymorphism predicts irinotecan toxicity: evolving proof. *AAPS Pharm Sci* 3: 2, 2001.
- Nagar S and Blanchard RL: Pharmacogenetics of uridine diphosphoglucuronosyltransferase (UGT) 1A family members and its role in patient response to irinotecan. *Drug Metab Rev* 38: 393-409, 2006.
- Innocenti F, Stadler WM, Iyer L, Ramirez J, Vokes EE and Ratain MJ: Flavopiridol metabolism in cancer patients is associated with the occurrence of diarrhea. *Clin Cancer Res* 6: 3400-3405, 2000.
- Boerner SA, Tourne ME, Kaufmann SH and Bible KC: Effect of P-glycoprotein on flavopiridol sensitivity. *Br J Cancer* 84: 1391-1396, 2001.
- Nakanishi T, Karp JE, Tan M, *et al*: Quantitative analysis of breast cancer resistance protein and cellular resistance to flavopiridol in acute leukemia patients. *Clin Cancer Res* 9: 3320-3328, 2003.
- Jager W, Zembsch B, Wolschann P, *et al*: Metabolism of the anticancer drug flavopiridol, a new inhibitor of cyclin dependent kinases, in rat liver. *Life Sci* 62: 1861-1873, 1998.
- Dobson PD and Kell DB: Carrier-mediated cellular uptake of pharmaceutical drugs: an exception or the rule? *Nat Rev Drug Discov* 7: 205-220, 2008.
- Hagenbuch B and Gui C: Xenobiotic transporters of the human organic anion transporting polypeptides (OATP) family. *Xenobiotica* 38: 778-801, 2008.
- Kim RB: Organic anion-transporting polypeptide (OATP) transporter family and drug disposition. *Eur J Clin Invest* 33 (Suppl 2): 1-5, 2003.
- Tamai I, Nezu J, Uchino H, *et al*: Molecular identification and characterization of novel members of the human organic anion transporter (OATP) family. *Biochem Biophys Res Commun* 273: 251-260, 2000.
- Muto M, Onogawa T, Suzuki T, *et al*: Human liver-specific organic anion transporter-2 is a potent prognostic factor for human breast carcinoma. *Cancer Sci* 98: 1570-1576, 2007.
- Wlcek K, Svoboda M, Thalhammer T, Sellner F, Krupitza G and Jaeger W: Altered expression of organic anion transporter polypeptide (OATP) genes in human breast carcinoma. *Cancer Biol Ther* 7: 1452-1457, 2008.
- Obaidat A, Roth M and Hagenbuch B: The expression and function of organic anion transporting polypeptides in normal tissues and in cancer. *Annu Rev Pharmacol Toxicol* 52: 135-151, 2012.
- Mikkaichi T, Suzuki T, Tanemoto M, Ito S and Abe T: The organic anion transporter (OATP) family. *Drug Metab Pharmacokinet* 19: 171-179, 2004.
- Abe T, Unno M, Onogawa T, *et al*: LST-2, a human liver-specific organic anion transporter, determines methotrexate sensitivity in gastrointestinal cancers. *Gastroenterology* 120: 1689-1699, 2001.
- Okabe M, Unno M, Harigae H, *et al*: Characterization of the organic cation transporter SLC22A16: a doxorubicin importer. *Biochem Biophys Res Commun* 333: 754-762, 2005.
- Ciarimboli G, Ludwig T, Lang D, *et al*: Cisplatin nephrotoxicity is critically mediated via the human organic cation transporter 2. *Am J Pathol* 167: 1477-1484, 2005.
- Yonezawa A, Masuda S, Yokoo S, Katsura T and Inui K: Cisplatin and oxaliplatin, but not carboplatin and nedaplatin, are substrates for human organic cation transporters (SLC22A1-3 and multidrug and toxin extrusion family). *J Pharmacol Exp Ther* 319: 879-886, 2006.
- Zhang S, Lovejoy KS, Shima JE, *et al*: Organic cation transporters are determinants of oxaliplatin cytotoxicity. *Cancer Res* 66: 8847-8857, 2006.
- Svoboda M, Wlcek K, Taferner B, *et al*: Expression of organic anion-transporting polypeptides 1B1 and 1B3 in ovarian cancer cells: relevance for paclitaxel transport. *Biomed Pharmacother* 65: 417-426, 2011.
- Okabe M, Szakacs G, Reimers MA, *et al*: Profiling SLCO and SLC22 genes in the NCI-60 cancer cell lines to identify drug uptake transporters. *Mol Cancer Ther* 7: 3081-3091, 2008.
- Ni W, Ji J, Dai Z, *et al*: Flavopiridol pharmacogenetics: clinical and functional evidence for the role of SLCO1B1/OATP1B1 in flavopiridol disposition. *PLoS One* 5: e13792, 2010.

34. Gui C, Miao Y, Thompson L, *et al*: Effect of pregnane X receptor ligands on transport mediated by human OATP1B1 and OATP1B3. *Eur J Pharmacol* 584: 57-65, 2008.
35. Treiber A, Schneider R, Hausler S and Stieger B: Bosentan is a substrate of human OATP1B1 and OATP1B3: inhibition of hepatic uptake as the common mechanism of its interactions with cyclosporin A, rifampicin, and sildenafil. *Drug Metab Dispos* 35: 1400-1407, 2007.
36. Leuthold S, Hagenbuch B, Mohebbi N, Wagner CA, Meier PJ and Stieger B: Mechanisms of pH-gradient driven transport mediated by organic anion polypeptide transporters. *Am J Physiol Cell Physiol* 296: C570-C582, 2009.
37. Murias M, Miksits M, Aust S, *et al*: Metabolism of resveratrol in breast cancer cell lines: impact of sulfotransferase 1A1 expression on cell growth inhibition. *Cancer Lett* 261: 172-182, 2008.
38. Riha J, Brenner S, Bohmdorfer M, *et al*: Resveratrol and its major sulfated conjugates are substrates of organic anion transporting polypeptides (OATPs): impact on growth of ZR-75-1 breast cancer cells. *Mol Nutr Food Res* 58: 1830-1842, 2014.
39. Palermo DP, DeGraaf ME, Marotti KR, Rehberg E and Post LE: Production of analytical quantities of recombinant proteins in Chinese hamster ovary cells using sodium butyrate to elevate gene expression. *J Biotechnol* 19: 35-47, 1991.
40. Unger C, Popescu R, Giessrigl B, *et al*: An apolar extract of *Critonia morifolia* inhibits c-Myc, cyclin D1, Cdc25A, Cdc25B, Cdc25C and Akt and induces apoptosis. *Int J Oncol* 40: 2131-2139, 2012.
41. Vavricka SR, Van Montfoort J, Ha HR, Meier PJ and Fattinger K: Interactions of rifamycin SV and rifampicin with organic anion uptake systems of human liver. *Hepatology* 36: 164-172, 2002.
42. Annaert P, Ye ZW, Stieger B and Augustijns P: Interaction of HIV protease inhibitors with OATP1B1, 1B3, and 2B1. *Xenobiotica* 40: 163-176, 2010.
43. Ji J, Mould DR, Blum KA, *et al*: A pharmacokinetic/pharmacodynamic model of tumor lysis syndrome in chronic lymphocytic leukemia patients treated with flavopiridol. *Clin Cancer Res* 19: 1269-1280, 2013.
44. Wong CC, Akiyama Y, Abe T, Lippiat JD, Orfila C and Williamson G: Carrier-mediated transport of quercetin conjugates: involvement of organic anion transporters and organic anion transporting polypeptides. *Biochem Pharmacol* 84: 564-570, 2012.
45. Wlcek K, Svoboda M, Thalhammer T, Sellner F, Krupitza G and Jaeger W: Altered expression of organic anion transporter polypeptide (OATP) genes in human breast carcinoma. *Cancer Biol Ther* 7: 1450-1455, 2008.
46. Carlson BA, Dubay MM, Sausville EA, Brizuela L and Worland PJ: Flavopiridol induces G1 arrest with inhibition of cyclin-dependent kinase (CDK) 2 and CDK4 in human breast carcinoma cells. *Cancer Res* 56: 2973-2978, 1996.
47. Baumann KH, Kim H, Rinke J, Plaum T, Wagner U and Reinartz S: Effects of alvocidib and carboplatin on ovarian cancer cells in vitro. *Exp Oncol* 35: 168-173, 2013.
48. Buxhofer-Ausch V, Secky L, Wlcek K, *et al*: Tumor-specific expression of organic anion-transporting polypeptides: transporters as novel targets for cancer therapy. *J Drug Deliv* 2013: 863539, 2013.
49. Seithel A, Eberl S, Singer K, *et al*: The influence of macrolide antibiotics on the uptake of organic anions and drugs mediated by OATP1B1 and OATP1B3. *Drug Metab Dispos* 35: 779-786, 2007.
50. Matsushima S, Maeda K, Ishiguro N, Igarashi T and Sugiyama Y: Investigation of the inhibitory effects of various drugs on the hepatic uptake of fexofenadine in humans. *Drug Metab Dispos* 36: 663-669, 2008.
51. Wang X, Wolkoff AW and Morris ME: Flavonoids as a novel class of human organic anion-transporting polypeptide OATP1B1 (OATP-C) modulators. *Drug Metab Dispos* 33: 1666-1672, 2005.